ACADEMIA ROMÂNĂ
Revue Roumaine de Chimie
http://web.icf.ro/rrch/

Rev. Roum. Chim.,
2016, *61*(4-5), 433-440

Dedicated to Professor Alexandru T. Balaban on the occasion of his 85th anniversary

AN EXPERIMENTAL APPROACH FOR FINDING LOW COST ALTERNATIVE SUPPORT MATERIAL IN PEM FUEL CELLS

Adriana MARINOIU,[a] Claudia COBZARU,[b,*] Elena CARCADEA,[a] Mircea RACEANU,[a] Irina ATKINSON,[c] Mihai VARLAM[a] and Ioan STEFANESCU[a]

[a] National RD Institute for Cryogenics and Isotopic Technologies- ICIT, 4 Uzinei St., Rm. Vâlcea, Roumania
[b] "Gheorghe Asachi" Technical University of Iaşi, Faculty of Chemical Engineering and Environmental Protection D. Mangeron, 71, 70050, Roumania
[c] Institute of Physical Chemistry "Ilie Murgulescu" of the Roumanian Academy, 202 Spl. Independenței, 060021 Bucharest, Roumania

Received November 16, 2015

PEM fuel cells have demonstrated their good energy efficiency and high power density per volume, but the high costs due to the noble metal catalysts, electrolyte membranes, and bipolar plates diminish the large scale marketing. Considering the potential of using graphene materials as low cost catalyst for the fuel cell applications, graphene nanocomposites were synthesized using a simple route by chemical oxidation and exfoliation of graphene oxide. The graphene nanocomposites obtaining was confirmed by characteristic analysis. Starting from graphite, the preparations of graphite oxide, graphene oxide, reduced graphene oxide and graphene–based nanocomposite**s**, as well as how to functionalize them with a compatible polymer, are described in this paper. The structure, morphology and properties were characterized during different preparation steps, using BET method, Scanning Electron Microscopy (SEM), Raman Spectroscopy, TGA analysis, XPS technique.

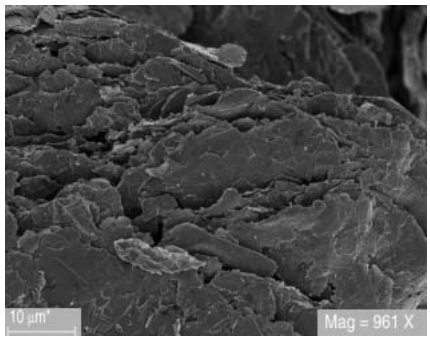

INTRODUCTION

In the perspective of a realistic commercial development, the proton exchange membrane fuel cells (PEMFCs) have attracted a considerable attention as a clean and efficient power source. For a successful PEMFC commercialization, the highly active and cost-effective electrodes (anode and cathode) are required for PEMFC commercialization.[1-6] Regarding the cathode materials, less-platinum cathodes such as carbon based materials have been proposed for PEMFC applications.

Currently, the most promising electrocatalyst for PEMFC is still platinum supported on carbon (Pt/C), because of the reliable electrochemical performance. Carbon-supported electrocatalysts are effective in upgrading the performance PEMFCs and reducing the use of precious metals, such as platinum Pt/C catalysts. Regarding this, considerable research efforts have been dedicated in order to develop durable catalyst support materials, such as carbon nanotubes, carbon molecular sieves and graphitic mesoporous carbon, due to their unique electric and micro- and macrostructure properties.[7-8] Nowadays, a durable

* Corresponding author: ccobzaru@yahoo.com

electrocatalyst based on graphene nanoplatelets as support, which exhibits 2–3 times durability of commercial Pt/C is the subject of many studies.[9]

Since the single-layer graphene was discovered, this research area has attracted great interest because it may lead to a new way to improve the electrocatalytic activity of catalyst used in fuel cells. [10-11] Si *et al.* reported that Pt can act as spacer for graphenes and lead to a potential high-surface-area material.[12]

In particular, graphene's high electrical conductivity and large surface area make it an interesting material for energy storage or conversion. A key issue is to develop advanced techniques in order to produce low cost and efficient graphene materials, by combining structural functions with superior electronic properties, having in mind the environmental context.

However, there are still some critical problems related to the investigation of graphene as catalysts support that needs to be further investigated. One of these, the functionalization with a compatible polymer in order to prepare the Pt/ graphene nanosheets is essential for fuel cell applications.

In this context, our paper main objective is to develop an easy and feasible method for synthesis of Pt supported on graphene materials. Starting from graphite, the preparations of graphite oxide (GO), graphene oxide (GrO), reduced GrO and graphene–based nanocomposite**s**, as well as how to functionalize them with a compatible polymer, in term of poly(diallyl dimethyl ammonium chloride) as compatible polymer, are described in this paper.

MATERIALS AND METHODS

In summary, the graphene nanosheets were obtained via a solution-based route, involving the chemical oxidation of graphite to graphite oxide (GO) by the Tour method. Graphite oxides were easily exfoliated to form graphene oxide sheets (GrO) by ultrasonication in water. The graphene oxide sheets were then reduced to graphene nanosheets (Gr) using sodium borohydride.

Purified natural graphite (PMM7) acquired from KOH–I-NOR Graphite SRO Czech Republic has the following characteristics: C = min. 99.5 %wt., ash = max. 0.5 %wt., specific surface = 9 m^2/g (BET). All other reagents and chemicals were procured from Sigma Aldrich, Alfa Aesar, Merck, and Fluka.

GO was prepared by the Tour method, for a high oxidation degree and a minimum unoxidized graphite, as was presented in our earlier report.[13] The graphite oxide is obtained after two stages: pre-oxidation and oxidation. In the pre-oxidation stage the H_2SO_4 was intercalated into graphite, to obtain a better access of the reactants in the oxidation step.

In the pre-oxidation step, the graphite was added slowly into a reaction mixture containing conc. H_2SO_4, $K_2S_2O_8$, P_2O_5, under continuous stirring. After heating up to 80°C and 4h at this reaction temperature, the mass was cooled down. The mixture was diluted in warm water and washed until pH 6, then was dried. In the oxidation stage, H_2SO_4, P_2O_5 and pre-oxidized graphite were added slowly, under stirring in an ice bath. After the suspension reached and maintaned the temperature level below 10°C, $KMnO_4$ were gradually added. After one hour, the reaction mass was gradually heated to 50°C and stirred. 35 wt% H_2O_2 was added until the solution turned to yellow. After filtration and washing repeteadly, the centrifugation and drying under vacuum were performed.

Few layer graphenes were obtained in the exfoliation stage, under specific conditions, namely 2 hours to 110W/40kHz at 30-40°C, in an ultrasonic bath. The pH of dispersed GO gel was corrected to 9-10 with Na_2CO_3 5 %wt. and reaction mass was stirred for 6 hours at the room temperature. In order to reduce GrO to the graphene, the colloidal solution of GrO, was added to a fresh $NaBH_4$ solution at 80°C and dosed under stirring in approx. 2 h. The reaction mass was maintained at 90°C for 4 hours, cooled to room temperature and separated by decantation and centrifugation. The separated solid was dried at 60°C, then was re-dispersed by sonication in H_2SO_4 and mechanically stirred for 12 hours at 120°C. After cooling, the reaction mass was washed with distilled water until free of SO_4^{2-}, filtered, washed with water and ethanol and dried at 80°C.

The obtaining of Pt/graphene nanocomposite involved getting the GO according to the above described procedure and then introducing of poly(diallyl dimethyl ammonium chloride) PDDA 20%wt. solution and H_2PtCl_6 8 %wt. in the exfoliating stage. The exfoliation was continued by sonication for 1.5 hours to 110W/40kHz at 30°C. Reaction mass was separated by centrifugation and the solid was washed. The reduction followed the steps from the above described procedure.

Characterization

The elemental analysis of the samples was determined by wavelength dispersive X-ray fluorescence (WDXRF) spectroscopy method. The Rigaku ZSX Primus II spectrometer is equipped

with an X-ray tube with Rh anode, 4.0 kW power, with front Be window of 30 μm thickness. The measurements were performed onto pressed pellets under vacuum. The XRF data were analyzed using EZ-scan combined with Rigaku's SQX fundamental parameters software (standard less) which is capable of automatically correcting for all matrix effects, including line overlaps. Raman spectra were recorded using a NRS-5100 Raman micro-spectrometer (Jasco Analytical Instruments, Japan). Trace metals (K, Mn) analysis was performed with an atomic absorption spectrometer VARIAN AA 240 FS after sample mineralization in a microwave digestion system MILLESTONE 1200 MEGA. For reliable and precise C, H, N, S and O determination, Thermo Scientific FLASH 2000 organic elemental analyzer was used together with argon as the carrier gas. The specific surface areas of the samples were determined using the BET method by performing nitrogen sorption measurements using a Quantachrome Autosorb IQ equipment. The adsorption and desorption experiments were done at 77 K after initial pre-treatment of the samples by degassing at 115°C for 4 hours. A simultaneous thermal-gravimetrical analyzer (device) SDT Q600 from TA Instruments was used. The samples were analyzed in the thermal rage 50-700^{o}C, with a temperature scanning rate 1^{o}C/min and the sample under continuous nitrogen flux, 100 ml/min, along the entire thermal scanning range. The weight lose with the increasing of the temperature was recorded. All experiments and characterization protocols were performed in order to reduce the possibility of error as much as possible, after the identification beforehand of significant sources of experimental errors.

RESULTS AND DISCUSSION

The structure, morphology and properties of prepared graphene materials were analyzed using different methods during various preparation steps.

The SEM micrograph from Fig. 1 emphasizes the morphology of typical structures derived from graphite, namely: graphite oxide (a) graphene (b), graphene nanocomposites (c), (d). The first intermediary product, named graphite oxide (GO), presents a structural deformation and surface irregularities, due to its chemical structure, specially the covalently oxygenated linking groups. The GO sample has large ordered crystallites as well as smaller disordered materials. The SEM micrograph shows the way GO agglomerates, as compact chunks and thin layers. Regarding the graphene materials, as can be seen, the flakes built a very good connected network which is crucial for the electronic transport for fuel cell applications. It is known the fact that in the powder form graphene sheets obtained from GO by most of the methods, have a wrinkled, fluffy and disordered morphology. In the specialty literature these structures have been named as graphene nanoplatelets or multi layer graphene.

The sheet nature of graphene is clearly identified from the SEM images. However, the graphene sheets are highly disordered and contain large amount of corrugations or wrinkles on their surface. These wrinkles are not point defects, but are extended surface defects as consequence of exfoliation process. The wrinkles can cause deviation from the sp^2/planar character expected for graphene. This aspect owns only to wrinkled graphene and no other carbon nanostructure. The morphology, nevertheless, confirms that these materials are graphene like materials and not amorphous carbons. In comparison, in the SEM images shown in figures 1(c) and (d) the graphene nano-composites sheets also appear to be arranged in a random and disordered three dimensional porous architecture.

Graphene sheets obtained by most of the methods have a wrinkled, fluffy and disordered morphology in the powder form. The graphene structures obtained by exfoliation of GO are associated as few layer wrinkled graphene. The BET surface area is obtained from the nitrogen adsorption–desorption isotherms shown in Fig. 2. The isotherms exhibit a typical type-IV curve at low relative pressure and a hysteresis loop at relative pressure from 0.4, indicating the presence of microporosity, mesoporosity, and some macroporosity. The high BET surface area of prepared graphene base materials (670 m^2/g) indicated a significant extent of exfoliation during the proposed technology. Nevertheless, the obtained BET surface area is less than values above 2000m^2/g for theoretical surface of individual separated graphene sheets.

The preparation of Pt/graphene nanocomposite involved the obtaining of GO according to the above described procedure in experimental part, followed by the introducing of conductor polymer, namely poly(diallyldimethylammonium chloride) PDDA 20%wt. solution and H_2PtCl_6 8 %wt. in the exfoliating stage.

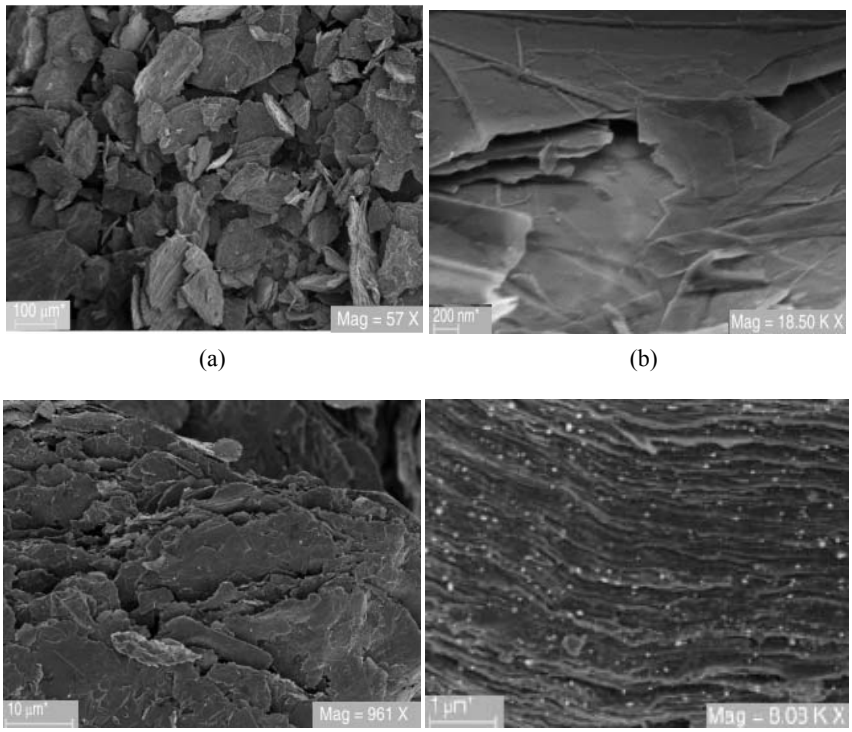

(a) (b)

(c) (d)

Fig. 1 – The SEM micrographs of the grafit oxide (a), graphene (b), graphene nanocomposites (c, d).

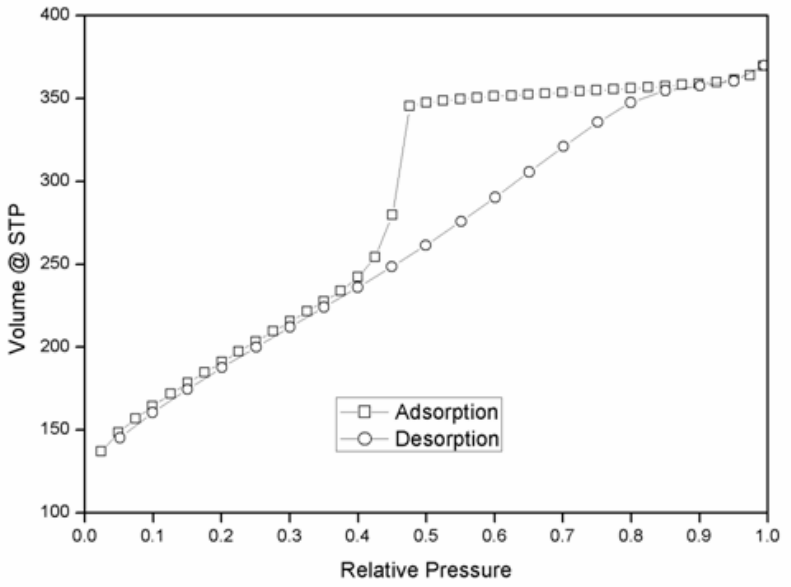

Fig. 2 – The adsorption–desorption isotherms for graphene.

Poly(diallyldimethylammoniumchloride) PDDA, known as cationic polyelectrolyte, can be adsorbed on the surface of carbon nanotubes or graphene through π–π and electrostatic interactions, and it could be used as a stabilizer for controlled synthesis of Pt/graphene. Graphene nanosheets with negative charge can be easily functionalized by positively charged PDDA through the electrostatic interaction, which can increase the stability of graphene in solution. On the other hand, $PtCl_6^{2-}$ ions can be confined in the positively charged surface of PDDA-functionalized graphene and then be *in situ* reduced to Pt nanoparticles upon the addition of reducing agents. Using this strategy, a controllable deposition of Pt nanoparticles on graphene could be performed. The Pt loading density can be effectively adjusted by changing the ratio of PDDA to the Pt precursor.

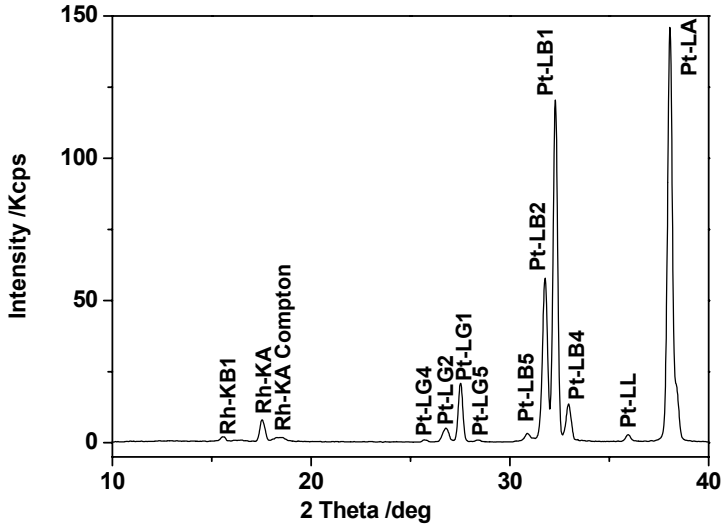

Fig. 3 – X-ray fluorescence spectrum of the Pt/graphene nanocomposite.

Table 1

Elemental composition of the Pt/graphene nanocomposite

Element	Result (mass %)	Det. Limit	El. Line
C	41.98	0.32	C -KA
O	12.44	0.95	O -KA
Pt	43.19	0.06	Pt-LA
Al	0.09	0.01	Al-KA
Si	0.35	0.01	Si-KA
S	0.13	0.02	S -KA
Cl	0.35	0.02	Cl-KA
Ca	0.11	0.02	Ca-KA
Fe	1.36	0.02	Fe-KA

Fig. 3 shows an overview of the Pt X-ray emission lines identified in the XRF spectrum of the Pt/graphene nanocomposite. The presence of Pt in the sample is confirmed through observation of L-series X-ray emission lines. Two strong peaks at 2θ 38.02° (Pt-LA) and 32.27° (Pt-LB1) beside smaller peaks corresponding to Pt-LB2-LB5 and Pt-LG1-LG5 are observed in the XRF spectrum. Table 1 presents the results obtained in the determination of C, O and Pt in the material analyzed in this study using SQX software. Besides C, O, Pt, other elements as impurities are observed in low amount.

Raman spectra are presented in Fig. 4. Two prominent peaks at 1594 and 1344 cm^{-1} corresponding to the G and D bands, respectively, are provided. The D/G relative high intensity ratio suggests a decreasing of sp^2-domain induced by reduction effect. PDDA acts as a p-type dopant to cause the partial electron-transfer from the electron-rich graphene substrate. The G band of graphene up-shifted at 1594 cm^{-1} indicates the occurrence of electron transfer from graphene to the charged N^+ centers of the adsorbed PDDA.[14-16] The intermolecular charge-transfer was supported by Raman spectroscopic measurements.[17-18] Similar G-band shifts caused by charge-transfer have been reported for graphene functionalized with other electron-accepting molecules.[19-20]

Thermal gravimetrical analysis (TGA) was performed for graphene and Pt/Graphene containing different PDDA amount as binder. The stages of weight loss are different for the mentioned samples. In the curve of Pt/ Graphene1(which contains 15% binder) can be noticed four stages of continuously weight loss until 480^{o}C. After this temperature the rate of weight loss remained almost constant. On the curve of Pt/Graphene2 sample (containing 10%

binder) there were only two stages of mass loss until 450°C. In the first stage under 120°C both samples lost water and light volatiles. Between 120 - 450°C the weight loss is due to PDDA backbone degradation.

The stability of Pt particles on the surface of graphene after heat treatment during the synthesis suggests a relatively strong interaction between graphene and Pt particles. The interaction between graphene and Pt may influence the electronic structure of Pt, and also possibly improve the performance of catalysts.

Fig. 6 showed the X-ray photoemission spectroscopy (XPS) results for prepared graphene materials. XPS analysis confirmed the presence of Pt in graphic materials.

The main peaks were attributed to Pt0 at 71.4 eV (4f7/2) and 74.7 eV (4f5/2), while 72.8, 76.2 and 75.0, 78.1 eV were assigned to Pt in 2^+ and 4^+ states, respectively. The results of different Pt species were calculated based on the above data and listed in Table 2. The relative intensity of Pt^0, Pt^{2+} and Pt^{4+} was calculated to be 82.02, 12.53 and 5.45% for Pt/graphene catalyst. It emphasizes a high degree of reduced to metallic Pt. By processing of XPS spectra, the following table was obtained.

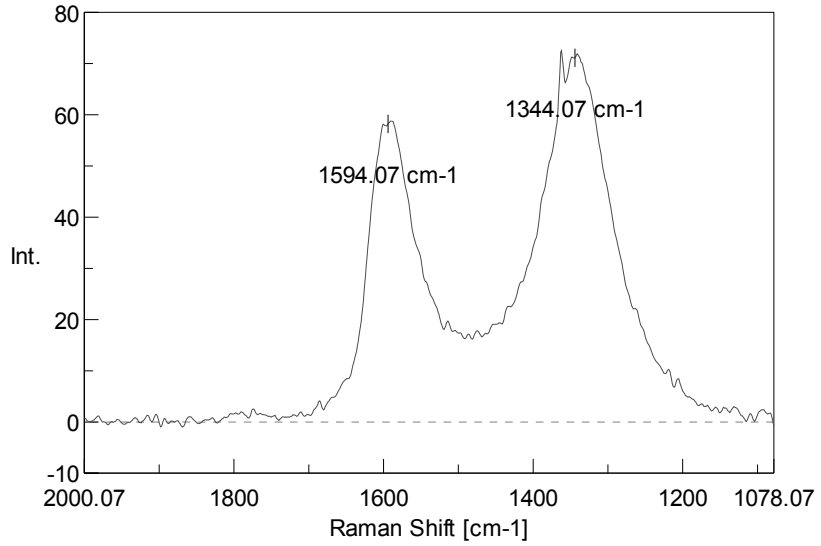

Fig. 4 – Raman spectra for Pt/graphene.

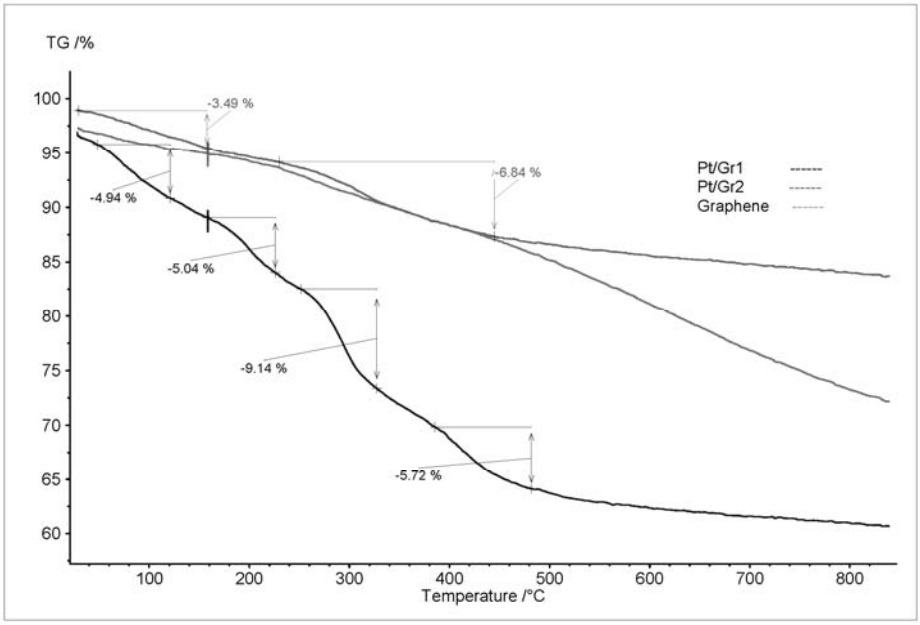

Fig. 5 – Thermogravimetric analysis of graphene and Pt/graphene.

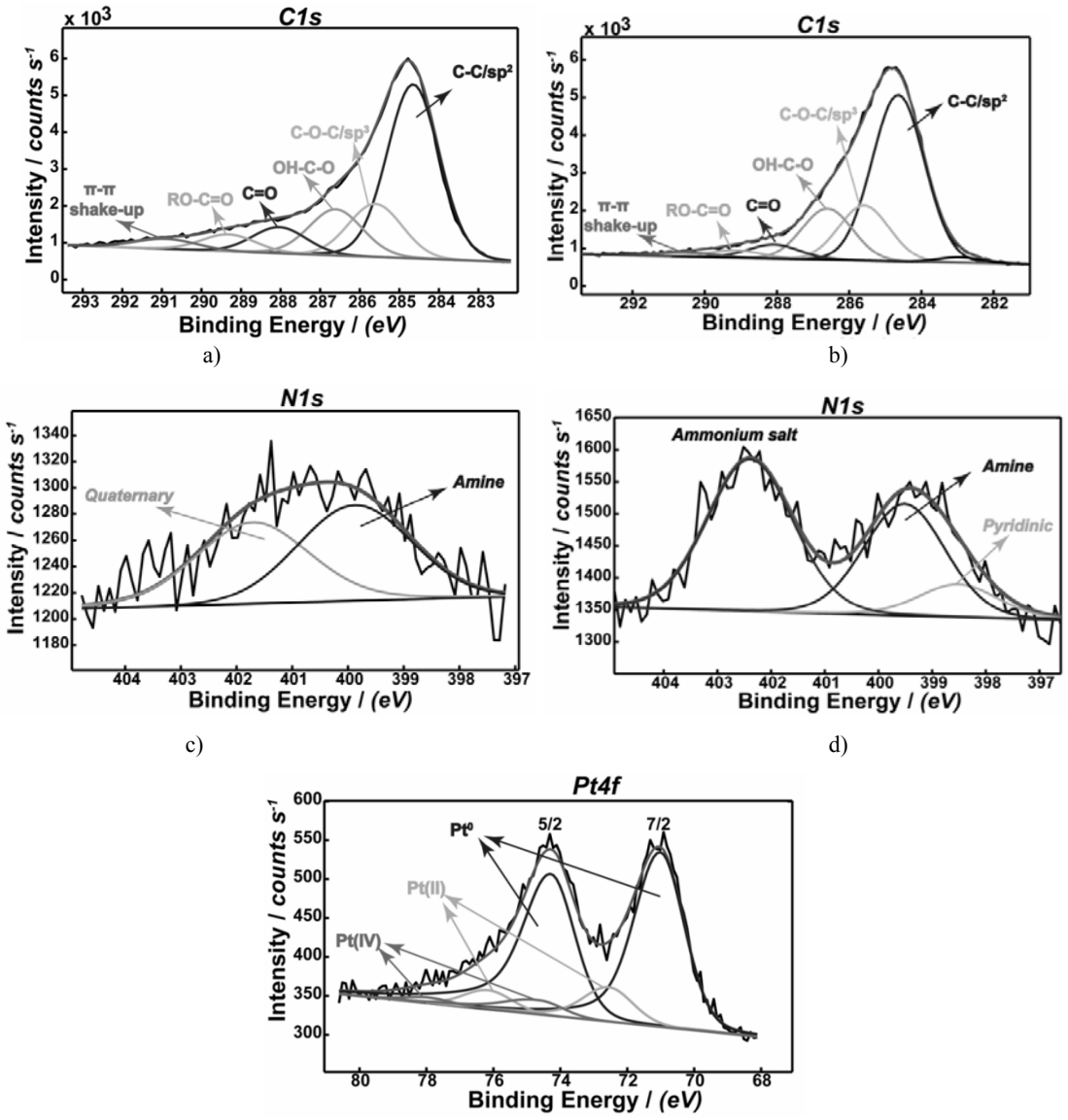

Fig. 6 – XPS C1s deconvoluted spectrum for graphene (a), XPS C1s deconvoluted spectrum for Pt/graphene, XPS N1s deconvoluted spectrum for graphene (c), XPS N1s deconvoluted spectrum for graphene (d), XPS Pt4f deconvoluted spectrum for Pt/graphene (e).

Table 2

X-ray photoemission spectroscopy results for graphene and Pt/graphene

Elements	Type of bond	Share of graphene (%)	Share of Pt/graphene (%)
C	C-C/sp2	52.47	55.47
	C-O-C/sp3	15.92	17.67
	HO-C-O	14.52	16.20
	C=O	8.17	4.91
	RO-C=O	5.39	2.63
	π-π shake-up	3.53	1.67
	pyridic	-	11.30

Table 2 (continued)

N	aminic	51.9	36.50
	quaternary	48.1	52.20
Pt	Pt	-	82.02
	Pt(II)	-	12.53
	Pt(IV)	-	5.45

The types of carbon links evidenced by photoelectron C1s deconvolution line are presented.The XPS spectrum of C(1s) shows different functional groups presented in samples: the non-oxygenated ring C (C–C, 285 eV), the C in C–O bond (C–O, 285.6 eV) and the carbonyl C (C O, 288.08 eV).

CONCLUSION

The aim of the paper was to demonstrated an easy and controllable process for obtaining platinum on graphene materials, using a simple approach. The high BET surface area indicated a significant degree of exfoliation during the proposed technology. The D/G relative high intensity ratio suggests a decrease of sp^2-domain induced by the reduction effect. Upon PDDA adsorption, the G band of graphene up-shifted at 1594 cm^{-1} indicates the occurrence of electron transfer from graphene to the charged N^+ centers of the adsorbed PDDA. The SEM micrographs revealed the presence of large, transparent graphene sheets with few layers. The SEM illustrates a rough surface structure for graphite oxide and a very good connected network for graphene materials, which certainly favors the electronic transport in the fuel cell applications.

Acknowledgment: This work is supported by the National Authority for Scientific Research and Innovation, Roumania, by the National Plan of R&D., Project no. PN 16 36 01 02 and by the Roumanian partnership in priority domains-PNII Programme, from MEN-UEFISCDI, under the project no 284/2014.

REFERENCES

1. S. Hong and S. Myung, *Nat. Nanotechn*., **2007**, *2*, 207-208.
2. C. A. Bessel, K. Laubernds, N. M. Rodriguez and R. T. K. Baker, *J. Phys. Chem. B.,* **2001**, *105*, 1115-1158.
3. A. L. Dicks, *J. Power Sources*, **2006**, *156*, 128-141.
4. M. J. Allen, V. C. Tung and R. B. Kaner, *Chem. Rev.*, **2010**, *110*, 132-145.
5. L. Qu, Y. Liu, J. B. Baek and L. Dai, *ACS Nano.*, **2010**, *4*, 1321-1326.
6. C. Casiraghi, A. Hartschuh, H. Qian, S. Pliscanec, C. Georgia, A. Fasoli, K. S. Novoselov, D.M. Basko and A.C. Ferrari, *Nano Letters*, **2009**, *9*, 1433-1441.
7. J. Campos-Delgado, J. M. Romo-Herrera, X . Jia, D. A. Cullen, H. Muramatsu, and Y. A. Kim, *Nano Letters*, **2008**, *8*, 2773-2778.
8. Y. Shaoa, S. Zhanga, C. Wanga, Z. Niea, J. Liua, Y. Wanga and Y. Lin, *J. Power Sources*, **2010**, *195*, 4600–4605
9. K. S. Novoselov, A. K. Geim, S. V. Morozov, D. Jiang, Y . Zhang, S. V. Dubonos, I.V. Grigorieva and A.A. Firsov, *Science,* **2004**, *306*, 666-669.
10. K. S. Novoselov, A. K. Geim, S. V. Morozov, D. Jiang, M. I. Katsnelson, I.V. Grigorieva, S. V. Dubonos and A.A. Firsov, *Nature,* **2005**, *438*, 197-200.
11. A. K. Geim and K. S. Novoselov, *Nat. Mater.,* **2007,** *6*, 183-191.
12. Y. C. Si, and E. T. Samulski, *Chem. Mater.,* **2008**, *20*, 6792–6797.
13. A. Marinoiu, C. Teodorescu, E. Carcadea, M. Raceanu, M. Varlam, C. Cobzaru, and I. Stefanescu, *Materials Today: Proceedings.,* **2015**, *2*, 3797-3805.
14. L. L. Zhang, R. Zhou and X. S. Zhao, *J. Mater. Chem.*, **2010**, 20, 5983–5992.
15. X. Qi, K.-Y. Pu, X. Zhou, H. Li, B. Liu, F. Boey, W. Huang, and H. Zhang, *Small,* **2010**, *6*, 663–669.
16. S. Wang, D. Yu, L. Dai, D. W. Chang and J. Baek, *ACS Nano*, **2011**, 5, 6202-6209.
17. J.-H Jang, D. Rangappa, Y.-U Kwon and I. Honma, *J. Mater. Chem.*, **2011**, 21, 3462–3466.
18. P. He and M. Bayachou, *Langmuir*, **2005**, 21, 6086–6092.
19. A. M. Rao, P.C. Eklund, S. Bandow, A. Thess, and R.E. Smalley, *Nature*, **1997**, 388, 257–259.
20. A. Marinoiu, M. Raceanu, E. Carcadea, D. Marinescu, C. Teodorescu, A.Melicchio, M. Varlam and I. Stefanescu, *React.Kinet.Mech.Cat*., **2016**, DOI 10.1007/s11144-016-0999-4.